Simulation study of Fermi level depinning in metal-MoS_2 contacts

P. Khakbaz[1], F. Driussi[1], P. Giannozzi[1, 2], A. Gambi[1], D. Esseni[1]

[1]*Università degli Studi di Udine, via delle Scienze 206, 33100 Udine, Italy*

[2]*CNR-IOM, Istituto dell'Officina dei Materiali, SISSA, I-34136 Trieste, Italy*

E-mail address of corresponding author: Khakbaz.Pedram@spes.uniud.it

Abstract

We used Density Functional Theory (DFT) to study the Fermi level pinning and Schottky barrier height in metal-MoS_2 contacts. We showed that the Fermi level de-pinning could be attained by controlling the distance between the metal and MoS_2. In particular, with proper buffer layers and the use of back-gated structures, the Schottky barrier height can be practically zeroed in some metal-MoS_2 stacks, which is important to attain Ohmic contacts.

1. Introduction and summary

Among 2D transition metal dichalcogenides, MoS_2 is the most technologically mature semiconductor [1]. Thanks to its extreme flexibility and large piezo-resistance [2], MoS_2 has great potentials for tactile sensing in soft robotics [3], for electronic skin [4] and fast thermal sensors [5], besides applications in nanoelectronic circuits [6]. But for most applications the quality of the metal-MoS_2 contact is critical, with best reported values being in the kΩ·μm range [6], which sharply contrasts with the projections of the IRDS roadmap [7], targeting tens of Ω·μm for nanoscale FETs.

The lack of dangling bonds at the MoS_2 surface may raise expectations for a weak Fermi level pinning (FLP) at the metal-MoS_2 interface and, thus, for a good control of the Schottky barrier height (SBH) with the metal work function (WF). However, the slope of the SBH versus WF curves has been experimentally reported to be as small as 0.09 [8]. Moreover, calculations based on Density Functional Theory (DFT) predict large densities of interface gap states (IGS) [9, 10], which are presumably responsible for the measured FLP.

In this paper, we report methodological guidelines and new DFT results for FLP and SBH in metal-MoS_2 contacts. We discuss the conditions for Fermi level de-pinning, which is a prerequisite for an engineering of the SBH and the attainment of an Ohmic behavior of the metal-MoS_2 contacts.

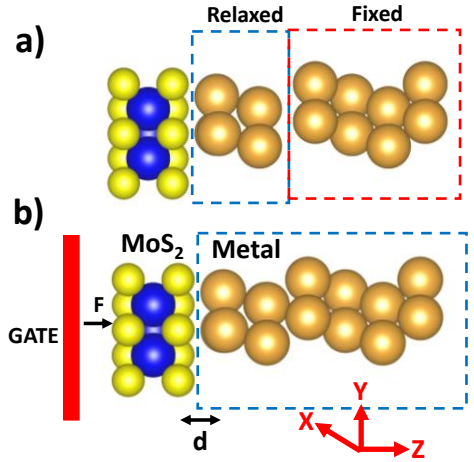

Fig. 1 : Simulation methods: ***(a)*** *as in [9, 10], four metal layers are fixed and the two metal layers adjacent to MoS_2 are relaxed.* ***(b)*** *This work: fully relaxed stack. Here d is the metal-MoS_2 distance. A back gate is included to bias the system.*

2. Simulation methodology and its validation

Quantum ESPRESSO is used to study the MoS_2 contacts with DFT [11]. The 111-surface of a six-layer metal crystal (Al or Au) is matched to a $\sqrt{3} \times \sqrt{3}$ MoS_2 monolayer supercell (*x*-*y* plane, Fig. 1) so as to minimize strain **[**10**]**, and then relaxation is used to reduce residual forces on atoms [12]. The supercell includes a 1.5 nm thick vacuum region along *z* (Fig. 1) and we used dipole correction to minimize the spurious coupling with periodic replicas of the supercell [11]. We employed Projector augmented-wave (PAW) pseudopotentials to describe electron−ion interactions and the Perdew−Burke−Ernzerhof (PBE) generalized gradient approximation (GGA) for the exchange and correlation functionals**.** Semi-empirical van der Waals corrections are included using DFT-D3 method. A back-gate is used to apply an electric field to the heterostructure along the *z* direction (Fig. 1b) [13, 14, 15].

Simulations fixing the position of the four top metal layers are reported in literature [9, 10], where only the two metal layers close to MoS_2 are relaxed (Fig. 1a). However, this may lead to artifacts in the dipole analysis. In fact, the dipole correction procedure uses an energy step (ΔV) to zero the field in vacuum [11]. Such ΔV value is often considered a measure of the charging of MoS_2 and it is also used to calculate the SBH [10]. But in the setup of Fig. 1a), the Au slab alone (MoS_2 is removed) has a sizeable ΔV in vacuum (black line, Fig. 2a), because of the mixture between fixed and relaxed atomic positions. The spurious ΔV of Au alone affects the ΔV and the SBH of the entire MoS_2-Au stack (red line), which has sometimes led to an overlooked artifact [9, 10].

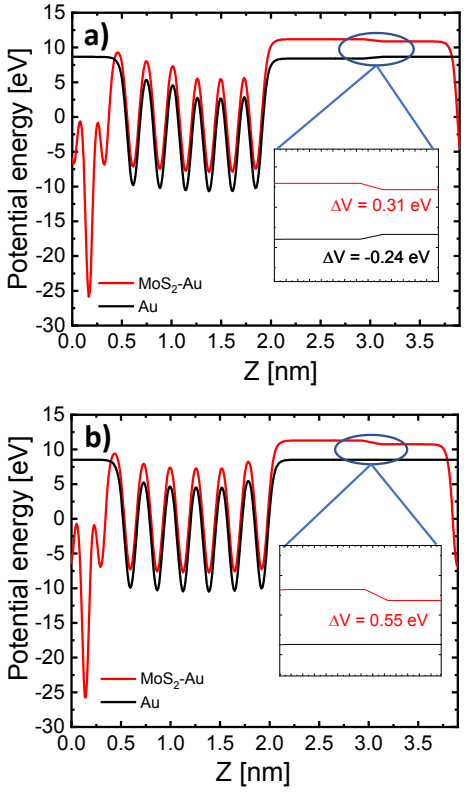

Fig. 2: Potential energy profiles of either Au alone or the MoS_2-Au stack. Steps in vacuum are used to zero the electric field due to dipoles in the stack. ***(a)*** *Simulations as in Fig.* ***1a)****, where the non-homogeneous Au alone displays dipole effects (black line), affecting also the MoS_2-Au result (red line).* ***(b)*** *Results from the simulations as in Fig.* ***1b)****. Au alone does not display any dipole effect.*

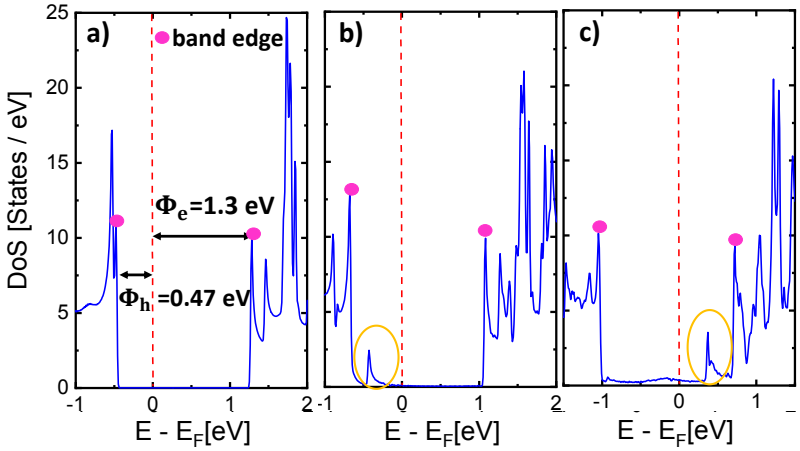

*Fig. 3: PDoS of MoS_2 in the MoS_2-Au stack for **(a)** d=0.8 nm, **(b)** d=0.4 nm and **(c)** d=0.3 nm (MD). At short distances and, in particular at the MD, we see the onset of IGS (e.g. the large peaks marked by the yellow oval) that pin the Fermi level E_F inside the bandgap.*

A more dependable procedure consists in relaxing the position of all atoms (Fig. 1b), and it has been used throughout this work. The Au slab alone now shows ΔV=0 in vacuum (black, Fig. 2b). Thus the ΔV value of the entire MoS_2-Au stack (red) is a genuine signature of the dipole in the contact. Minimum energy distances (MD) between MoS_2 and Au (0.3 nm) or Al (0.27 nm) are obtained upon stack relaxation [10]. The calculated band structures of separated MoS_2, Au and Al have been also verified against literature data (not shown).

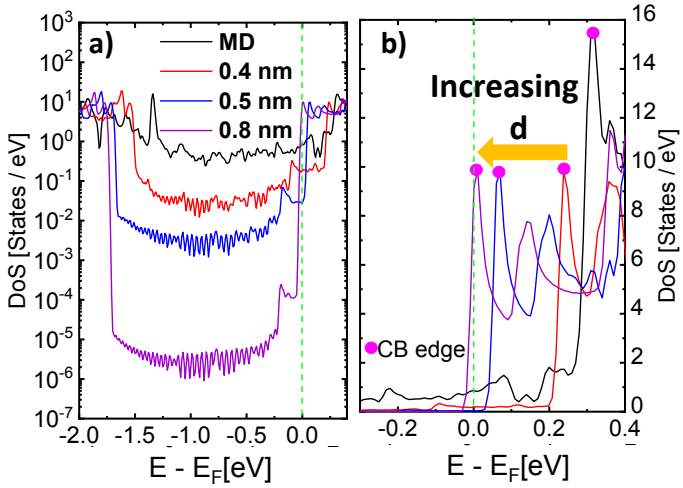

*Fig. 4: PDoS of MoS_2 in MoS_2-Al stack for different d values in logarithmic **(a)** and linear scales **(b**, zoomed around E_F). For MD, E_F is pinned in the MoS_2 bandgap due to IGS (black). By increasing d, the IGS density is suppressed, so that E_F gets depinned and reaches the MoS_2 CB for d=0.8 nm.*

3. Fermi level pinning and interface states

To evaluate the SBH and FLP, the partial density of states (PDoS) of MoS_2 is extracted for different distances, *d*, between MoS_2 and Au (Fig. 1). For *d*=0.8 nm (Fig. 3a), the PDoS of the MoS_2 layer is consistent with the isolated material (E_{gap} ≈ 1.8 eV), with no IGS. Moreover, by defining the SBH for electrons/holes (Φ_e / Φ_h) as the difference between the conduction/valence band (CB/VB) edge and the Fermi level (E_F), the extracted SBH agrees well with the Schottky–Mott rule with a work function WF=5.5 eV for Au and a MoS_2 affinity of 4.2 eV. For shorter *d* values (Fig. 3b and c), instead, the IGS density increases considerably, thus pinning E_F and affecting the SBH. Similar results are observed for the MoS_2-Al stack (Fig. 4), with a large PDoS increase in the MoS_2 gap at small *d* (a), that pins E_F. For *d*=0.8 nm, instead, the SBH is about zero, consistently with WF=4 eV for the Al slab.

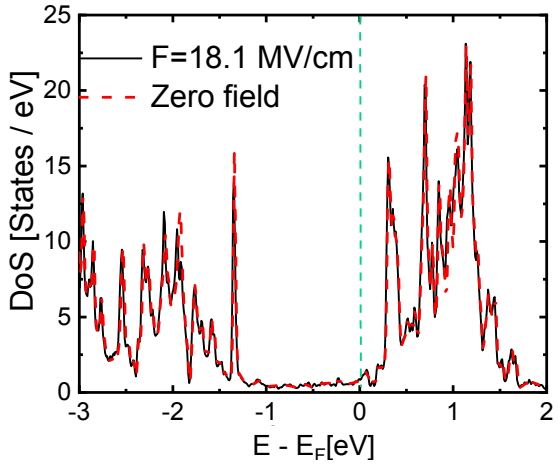

Fig. 5: PDoS of MoS_2 in the back gated MoS_2-Al stack at MD for F=0 and 18.1 MV/cm. E_F is strongly pinned and the electric field imposed by the back gate cannot influence E_F.

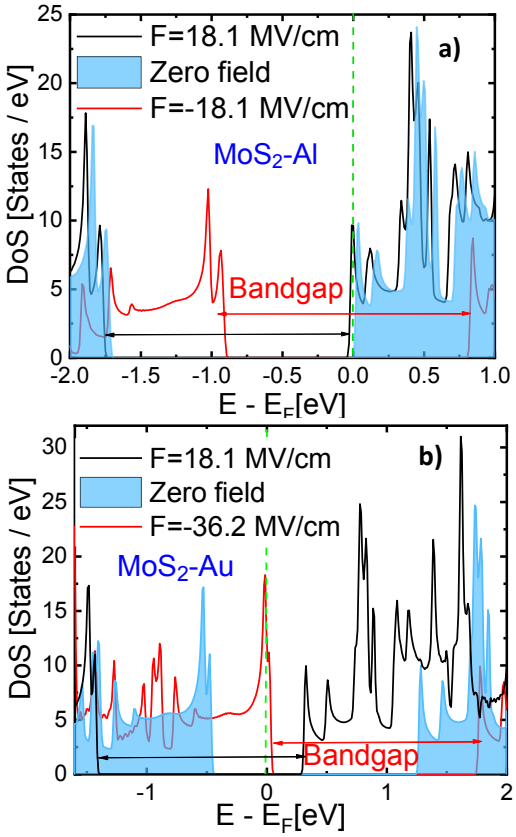

*Fig. 6: **(a)** PDoS of MoS_2 in back gated MoS_2-Al at d=0.8 nm. E_F is de-pinned: the field shifts E_F with respect to CB and VB of MoS_2 (n-type contact for F>0). **(b)** PDoS in MoS_2-Au at d=0.8 nm. The field shifts E_F inside the MoS_2 bandgap (p-type contact for F=-36.2 MV/cm).*

4. Back gated MoS_2 contacts

The back-gate in Fig. 1b) allows the biasing of MoS_2 through an external electric field (F). However, the strong FLP for small d values precludes any SBH modulation (Fig. 5). For d=0.8 nm, instead, due to the E_F depinning, the field can shift E_F with respect to the CB edge (Fig. 6), hence Φ_e reduces for F>0 and increases for F<0. To gain a better physical insight, we extracted the F induced charge in MoS_2 by using either the Bader analysis [13, 16] or simply the Gauss law; in fact, for d=0.8 nm, a dependable F value can be determined at both sides of MoS_2 from the potential energy profile (Fig. 7).

The charges extracted from Bader analysis or Gauss law agree well for MoS_2-Al (Fig. 8a) and MoS_2-Au (b). An electric field $F > 0$ increases the electron density in MoS_2 and eases the contact to the CB in the MoS_2-Al system, while a negative field eases a contact to the VB in the MoS_2-Au stack. It is worth mentioning that the apparently large F values needed to induce n-type or p-type contacts are due to the use of vacuum as a spacer between MoS_2 and the back-gate. By exploiting the dielectrics typically available in CMOS technologies, the required field can be reduced by a factor equal to the corresponding permittivity, namely of about 4 for SiO_2 and 30 for HfO_2.

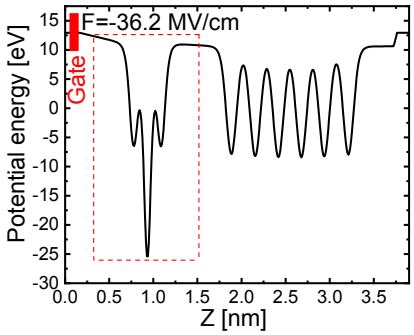

Fig. 7: Back gated MoS_2-Au stack. d=0.8 nm is large enough to calculate the field at both sides of MoS_2 (red dashed box).

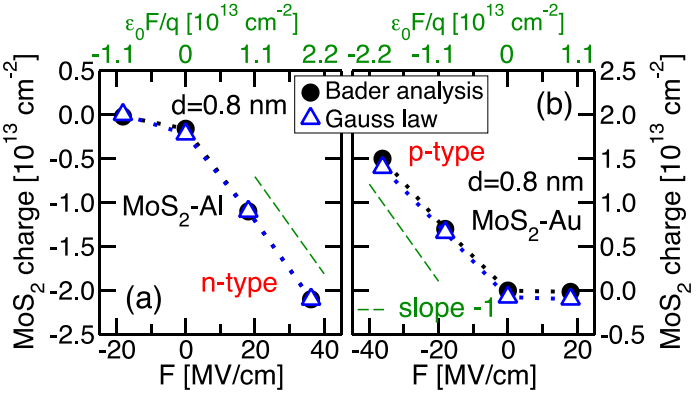

*Fig. 8: MoS_2 charge vs. F extracted with Bader analysis or through the Gauss law for MoS_2-Al **(a)** and MoS_2-Au **(b)** stacks. The back gate field induces either a n-type **(a)** or a p-type contact **(b)**.*

5. Conclusions

The reported DFT results for FLP and SBH provide useful insights for the attainment of an Ohmic metal-MoS_2 contacts. The control of the distance *d* is crucial in order to enable a modulation of the SBH, that can be further adjusted by an effective back-gating of the structure. This may be achieved thanks to the insertion of a proper buffer layer such as graphene or h-BN between the metal and MoS_2. Such a possible engineering of the metal-MoS_2 contacts has been in fact explored in the recent literature, with some preliminary but encouraging results [17, 18].

Acknowledgments

This work was supported by the Italian MIUR through the PRIN Project 2017SRYEJH and by the European Union through the MaX Center of Excellence (Grant No. 676598).

References

[1] Radisavljevic B, Radenovic A, Brivio J, Giacometti V, Kis A. Single-layer MoS_2 transistors. Nature nanotechnology. 2011 Mar;6(3):147-50.

[2] Hosseini M, Elahi M, Pourfath M, Esseni D. Strain-Induced Modulation of Electron Mobility in Single-Layer Transition Metal Dichalcogenides MX_2 (M = Mo, W; X = S, Se). IEEE Transactions on Electron Devices. 2015 Aug 10;62(10):3192-8.

[3] Rus D, Tolley MT. Design, fabrication and control of soft robots. Nature. 2015 May;521(7553):467-75.

[4] Chortos A, Liu J, Bao Z. Pursuing prosthetic electronic skin. Nature materials. 2016 Sep;15(9):937-50.

[5] Khan A.I., Khakbaz P, Brenner K.A., Smithe K.K., Mleczko M.J., Esseni D., Pop E. Large temperature coefficient of resistance in atomically thin two-dimensional semiconductors. Applied Physics Letters. 2020 May 18;116(20):203105.

[6] Iannaccone G, Bonaccorso F, Colombo L, Fiori G. Quantum engineering of transistors based on 2D materials heterostructures. Nature nanotechnology. 2018 Mar;13(3):183-91.

[7] International Roadmap for Devices and Systems (IRDS), [online] Available: http://irds.ieee.org/.

[8] Kim C, Moon I, Lee D, Choi MS, Ahmed F, Nam S, Cho Y, Shin HJ, Park S, Yoo WJ. Fermi level pinning at electrical metal contacts of monolayer molybdenum dichalcogenides. ACS nano. 2017 Feb 28;11(2):1588-9.

[9] Kang J, Liu W, Sarkar D, Jena D, Banerjee K. Computational study of metal contacts to monolayer transition-metal dichalcogenide semiconductors. Physical Review X. 2014 Jul 14;4(3):031005.

[10] Farmanbar M, Brocks G. First-principles study of van der Waals interactions and lattice mismatch at MoS_2/metal interfaces. Physical Review B. 2016 Feb 2;93(8):085304.

[11] Giannozzi P, et al. Advanced capabilities for materials modelling with Quantum ESPRESSO. Journal of Physics: Condensed Matter. 2017 Oct 24;29(46):465901.

[12] Zhong H, Quhe R, Wang Y, Ni Z, Ye M, Song Z, Pan Y, Yang J, Yang L, Lei M, Shi J. Interfacial properties of monolayer and bilayer MoS_2 contacts with metals: beyond the energy band calculations. Scientific reports. 2016 Mar 1 ;6(1) :1-6.

[13] Driussi F, Venica S, Gahoi A, Gambi A, Giannozzi P, Kataria S, Lemme MC, Palestri P, Esseni D. Improved understanding of metal–graphene contacts. Microelectronic Engineering. 2019 Aug 15; 216:111035.

[14] Khakbaz P, Driussi F, Gambi A, Giannozzi P, Venica S, Esseni D, Gaho A, Kataria S, Lemme M. C. DFT study of graphene doping due to metal contacts. Proceedings of SISPAD. September 2019. 1-4.
[15] Brumme T, Calandra M, Mauri F. Electrochemical doping of few-layer ZrNCl from first principles: Electronic and structural properties in field-effect configuration. Physical Review B. 2014 Jun 6;89(24):245406.
[16] Henkelman G, Arnaldsson A, Jónsson H. A fast and robust algorithm for Bader decomposition of charge density. Computational Materials Science. 2006 Jun 1;36(3):354-60.
[17] Farmanbar M, Brocks G. Ohmic contacts to 2D semiconductors through van der Waals bonding. Advanced electronic materials. 2016 Apr;2(4):1500405.
[19] Kaushik N, Karmakar D, Nipane A, Karande S, Lodha S. Interfacial n-doping using an ultrathin TiO_2 layer for contact resistance reduction in MoS_2. ACS applied materials & interfaces. 2016 Jan 13;8(1):256-63.